Novel cross-link breaker based on zwitterion structure: Synthesis, structure and druggability studies

ARTICLE *in* EUROPEAN JOURNAL OF MEDICINAL CHEMISTRY · AUGUST 2013

Impact Factor: 3.45 · DOI: 10.1016/j.ejmech.2013.07.033 · Source: PubMed

5 AUTHORS, INCLUDING:

Xin-Bo Zhou

17 PUBLICATIONS **53** CITATIONS

SEE PROFILE

Song Li

Southeast University (China)

189 PUBLICATIONS **2,601** CITATIONS

SEE PROFILE

Wu Zhong

Beijing Institute of pharmacology and toxic…

50 PUBLICATIONS **202** CITATIONS

SEE PROFILE

European Journal of Medicinal Chemistry 68 (2013) 89–95

Contents lists available at ScienceDirect

European Journal of Medicinal Chemistry

journal homepage: http://www.elsevier.com/locate/ejmech

Original article

Novel cross-link breaker based on zwitterion structure: Synthesis, structure and druggability studies☆

Shuang Cao [a,1], Xin-Bo Zhou [a,1], Heng Zhang [b], Song Li [a], Wu Zhong [a,*]

[a] Laboratory of Computer-Aided Drug Design & Discovery, Beijing Institute of Pharmacology and Toxicology, 27 Taiping Rd., Beijing 100850, China
[b] Hubei Key Laboratory of Novel Chemical Reactor and Green Chemical Technology, Wuhan Institute of Technology, Wuhan, Hubei 430073, China

ARTICLE INFO

Article history:
Received 24 May 2013
Received in revised form
2 July 2013
Accepted 5 July 2013
Available online 9 August 2013

Keywords:
Advanced glycosylation end-products (AGEs)
Cross-link breaker
Zwitterion
X-ray structure
Druggability
In situ IR

ABSTRACT

It has been universally acknowledged that the increase in cardiac and vascular stiffness is due to the formation of advanced glycosylation end-products (AGEs). Research on the stable form of 3-(carboxymethyl)-4-methylthiazol bromide sodium salt ($C_6H_7BrNNaO_2S$) showed that it had a notable effect on breaking the AGEs. Two compounds with novel structures, zwitterionic 3-(carboxymethyl)-4-methylthiazol ($C_6H_7O_2NS$) and a dipolymer ($C_{12}H_{15}O_4N_2S_2Br$) complex, were obtained. When compared with the forms of sodium salt and dipolymer, zwitterion had an obvious advantage in stability, solubility, synthesis and pH, which made the zwitterion a promising drug. The structure of sodium salt, dipolymer and zwitterion was comparatively analyzed by such methods as single crystal X-ray diffraction, ESI-MS, ^{1}H NMR, FT-IR and *in situ* IR.

1. Introduction

Excessive formation of advanced glycosylation end-products (AGEs) is a significant factor contributing to the development of cardiovascular diseases associated with aging, diabetes and hypertension as has been widely documented [1,2]. Glucose can react non-enzymatically with long-lived proteins, such as collagen and lens crystallin, linking them together to form cross-links, that will eventually generate advanced glycosylation end-products (AGEs). Formation of AGEs leads to increasing levels of oxidative stress, and their accumulation in serum, kidney and vascular tissues is a key risk marker for microvascular complications, especially in diabetic patients [3,4].

To decrease the number of these cross-links, some compounds have been discovered, the majority of which belong to a class of thiazolium derivatives such as phenacylthiazolium bromide (PTB) and ALT-711 [5–7]. These compounds can selectively cleave diketone bridges of two adjacent carbonyl groups that might form intermolecular cross-links with amino acid side chains and thus appears to reverse cross-linking both *in vitro* and *in vivo* [8–10].

Based on the principle of "cross-link breakers", we designed a series of *N*-(carboxymethyl) thiazolium derivatives [11,12]. By screening from these hundreds of betaines, some active candidates, having a common structure of ester, were identified. Subsequently, pharmacokinetic studies on these active candidates in our laboratory indicated that the functional ester group was predominantly metabolized into carboxyl *in vivo*. Therefore, we believe that these compounds play the role of "cross-link breaker".

According to the exact molecular mechanism, we reduced these *N*-(carboxymethyl) thiazolium derivatives, and designed the simplest representative of these derivatives, namely a 3-(carboxymethyl)-4-methylthiazol bromide sodium salt ($C_6H_7BrNNaO_2S$). The satisfactory efficacy of which *in vivo* had been confirmed by experiments performed in rats. However, to our great surprise, the results of X-ray analysis revealed that this compound including both sodium acetate and quaternary ammonium salt was not stable enough for isolation, possibly because the sodium and bromine cannot regularly exist in one molecule, a portion of which cohered in the form of NaBr. Subsequently, dipolymer ($C_{12}H_{15}O_4N_2S_2Br$) and zwitterion ($C_6H_7O_2NS$) were obtained by synthesis. After a series of

* Corresponding author.
E-mail address: zhongwu@bmi.ac.cn (W. Zhong).

[1] These authors contributed equally to this work.

0223-5234/$ – see front matter © 2013 The Authors. Published by Elsevier Masson SAS. All rights reserved.
http://dx.doi.org/10.1016/j.ejmech.2013.07.033

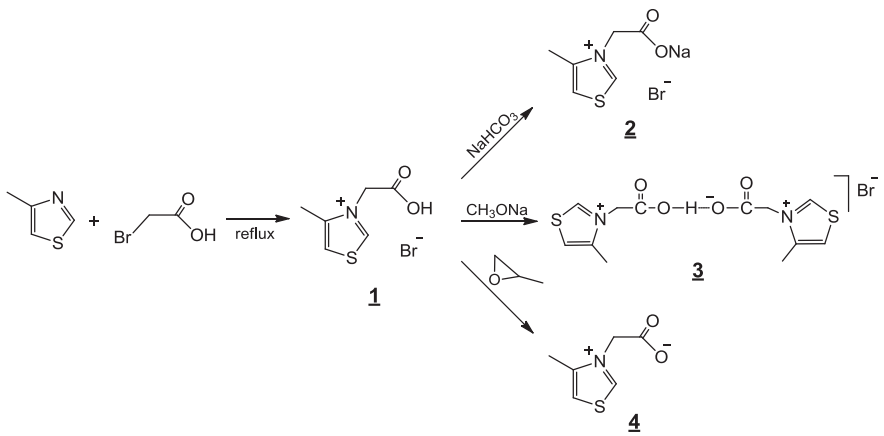

Scheme 1. Synthesis of compounds **2**–**4**.

comparative analyzes, we came to the conclusion that the zwitterion form has the most promising druggability of these potential "cross-link breakers".

To date although several zwitterions have been identified, an overwhelming majority of them stably exist in the form of coordination complexes [13,14]. Therefore, only a few of their structures have been determined in the solid state [15], so that there has been very little drug design based on zwitterionic structure appearing on the market. In this paper, a novel thiazole derivative, namely the zwitterionic 3-(carboxymethyl)-4-methylthiazol, which has a structure analogous to amino acid and a zwitterionic form containing a positively charged quaternary ammonium and a negatively charged carboxylate, is reported. Synthesis, structural characterizations and druggability studies of the three compounds will be described below.

2. Results and discussion

2.1. Synthetic studies

To determine the most stable structure of this "cross-link breaker", several syntheses are carried out and three forms of the target compounds (**2**–**4**) are obtained (Scheme 1). In the reaction to **2** and **3**, the quantity of base must be strictly restricted to the equimolar amount of the carboxylic derivation or else the redundant base would not be easily separated from the target sodium salt. In contrast to reactions 1 and 2, reaction 3 has the obvious predominance in outcome and refinement.

2.2. Structural studies

2.2.1. X-ray crystallography

The crystal data and details of structure refinement of compounds **2**–**4** are given in Table 1.

The asymmetric unit is shown in Fig. 1. In the single crystal structure of **2**, two donor sites of one ligand link to the sodium cation, Na2, via the coordination bond Na2–O3 and Na2–O4 (Na2–O3 = 2.530(6) Å and Na2–O4 = 2.410(6) Å), while the two donor sites coming from different ligands connect to Na1 via coordination bond Na1–O3 and Na1–O1 (Na1–O3 = 2.336(7) Å and Na1–O1 = 2.351(7) Å). Although the two bromine atoms in this molecule are apparently isolated, the distance from bromine to sodium (Br1–Na1 = 2.869(3) and Br2–Na2 = 2.864(3) Å) suggests that there is a great probability of bonding between them.

Table 1
Crystallographic data and details of structure refinement of compounds **2**–**4**.

Complex	**2**	**3**	**4**
Empirical formula	$C_{12}H_{14}Br_2N_2Na_2O_4S_2$	$C_{12}H_{15}BrN_2O_4S_2$	$C_6H_7NO_2S{\bullet}H_2O$
Formula weight	520.20	395.29	175.2
Crystal system	Triclinic	Monoclinic	Orthorhombic
Space group	*P*2(1)/n	*P*2(1)/n	*P*2(1)/n
a (Å)	8.9000(18)	5.1907(10)	5.6082(11)
b (Å)	9.4095(19)	12.092(2)	8.4615(17)
c (Å)	12.028(2)	13.052(3)	16.064(3)
α (°)	92.82	90	90
β (°)	109.00	97.96	90
γ (°)	104.11	90	90
V [Å^{-3}]	914.5(3)	811.3(3)	762.3(3)
Z	2	2	4
ρ_{calcd} [Mg/m^3]	1.904	1.618	1.527
F(000)	520	400	368
Crystal size (mm)	0.40 × 0.30 × 0.10	0.20 × 0.10 × 0.10	0.20 × 0.18 × 0.10
θ range for data collection	2.25–25.03°	2.31–25.01°	2.54–27.89°
Limiting indices	$-10 \le h \le 10, -11 \le k \le 11, -14 \le l \le 14$	$-6 \le h \le 6, -14 \le k \le 14, -15 \le l \le 14$	$-7 \le h \le 6, -11 \le k \le 11, -21 \le l \le 21$
Reflections collected/unique	5591/3046 [*R*(int) = 0.0303	5418/1424 [*R*(int) = 0.0303]	8477/1822 [*R*(int) = 0.0403]
Temperature (K)	293(2)	113(2)	143(2)
Data/restraints/parameters	3046/4/217	1424/1/102	1822/0/110
Final *R* indices [$I > 2\delta(I)$]	$R_1 = 0.0509$	$R_1 = 0.0336$	$R_1 = 0.0266$
R indices (all data)	$wR_2 = 0.1391$	$wR_2 = 0.0851$	$wR_2 = 0.0645$
Largest diff. peak and hole (Å^{-3})	0.960 and −0.676	0.463 and −0.989	0.232 and −0.211

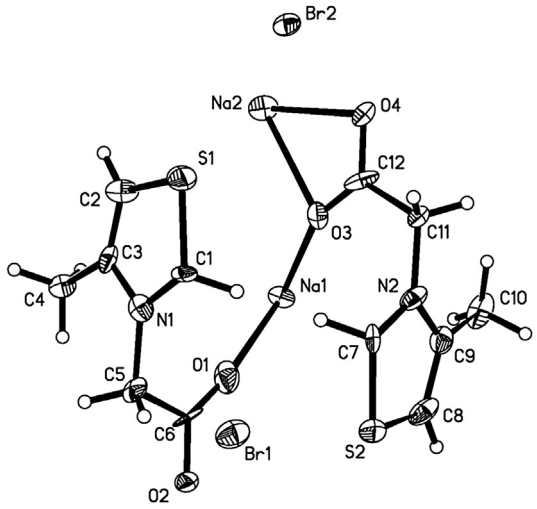

Fig. 1. The X-ray crystal structure of **2**, with displacement ellipsoids drawn at the 50% probability level.

X-ray diffraction data of complex **3** (Table 1) reveals a novel structure in which a proton (linked to an alternative zwitterion through the formation of a hydrogen bond) is shared by two zwitterion molecules; this structure is also in accordance with the elemental analysis [16,17]. The active proton is maintained moving between two zwitterions; when one bond distance of O2–H is 0.84(4), the other (O2A…H) is 1.62(4) Å (Table 2), with an O–H…O angle of 172(6)°, keeping conversion at all times (Table 2). The O–C–O angles of the carboxyl groups are 126.5°, with the bond length of the two O–C being 1.226(3) Å and 1.281(3) Å, respectively, while the skewness parameter of 0.055(3) Å shows that the crystal environment of the proton favors the O2 site (Fig. 2). In the mass spectrum data, the signal at $m/z = 158$ for the single acid unit is the most intense peak, but a dimeric cation at $m/z = 315$ is also observed.

The negative charge of *COO-*, *Br-* and two positive charged nitrogen atoms keep the charge balance in this hydrogen-bonded dimer. The result of this special structure may come from the weak acidic property of **3** that leads to a proton barely dissociating from the carboxylic acid.

In our attempt to react 4-methylthiazole with sodium bromoacetate, a compound inlaid in several water molecules (Fig. 3) is obtained. Due to the presence of unordered fragmentation in the water molecule, it is unlikely that the structure of this molecule can be unambiguously determined.

Table 2
Hydrogen bond lengths (Å) and bond angles (°) in **2**–**4**.

D–H…A	d(D–H)	d(H…A)	d(D…A)	∠(DHA)
2				
O(2)–H(2A)…S(2)[a]	0.851(5)	2.375(2)	3.227(6)	179.5(4)
O(4)–H(4A)…S(1)[b]	0.858(5)	2.388(3)	3.246(6)	179.4(4)
3				
O(2)–H(2)…O(2)[c]	0.84(4)	1.62(4)	2.451(4)	172(6)
4				
O(3)–H(3A)…O(1)	0.84(3)	1.96(3)	2.8014(18)	172(2)
O(3)–H(3B)…O(2)[d]	0.82(3)	2.07(3)	2.885(2)	178(2)
O(3)–H(3B)…O(1)[d]	0.82(3)	2.67(2)	3.2260(17)	127(2)

[a] Symmetry code: $-x, -y, -z$.
[b] Symmetry code: $-x, -y + 1, -z + 1$.
[c] Symmetry code: $-x + 2, -y + 2, -z + 1$.
[d] Symmetry code: $x - 1/2, -y + 1/2, -z + 1$.

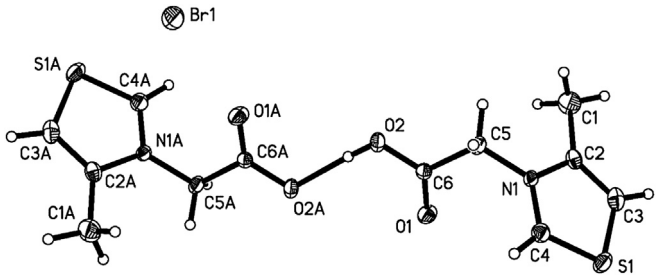

Fig. 2. The X-ray crystal structure of **3**, with displacement ellipsoids drawn at the 50% probability level.

Structure of **4**, an absolute zwitterion, without any extraneous component, is in good agreement with those measured by elemental analysis. This zwitterion is stabilized by charge delocalization (Fig. 4).

After a single crystal (Fig. 5) was obtained, it was puzzlingly determined to contain a water molecule and this has been verified by multiple experiments [18]. The thiazole ring is almost planar with a maximum displacement of 0.009 Å for the C3 atoms. The carboxymethyl group involving atoms C5, C6, O1 and O2 is located above the thiazole plane. Also, the C–COO^- group, which is also planar, intersects with the thiazole plane at an angle of 79.62° [16].

The bond lengths of C6–O1 (1.2525 Å) and C6–O2 (1.2530 Å) are very similar, with an O1–C6–O2 angle of 127.56°, which suggests the two atoms have identical chemical properties. The oxygen atoms, O1 and O2, are directed toward the hydrogen atoms of different water molecules with distances ranging from 1.96 to 2.07 Å, and hydrogen atoms linking C1 and C4 also interact weakly with the oxygen atoms of water by means of hydrogen bonding (Fig. 6). From what has been discussed above, we can reason that water molecules are absolutely indispensable to the formation of a stabilizing single crystal [19]. Some short C–H…O contacts presenting among layers of the two units as well as van der Waals forces between the oxygen and sulfur atoms of the next thiazole ring all contribute to the stabilization of the crystal structure [20].

In the mass spectrum, the signal at $m/z = 158$ $[M + H]^+$ for the single unit is the most intense peak, a dipolymer at $m/z = 315$ $[2M + H]^+$, and a trimerization at $m/z = 472$ $[3M + H]^+$ is also observed.

2.2.2. ^1H NMR spectroscopy

In particular, as structural change (from **1** to **3**, to **2**, to **4**), the chemical shifts of protons (H_{C1}, H_{C3} and H_{C5}) display a law of diminishing (Table 3). In DMSO, the ^1H chemical shift of these protons (Fig. 7) undergoes only minor changes on conversion of **1** to **3**, **2** and **4** except in the case of the proton linking to C5. The signal of

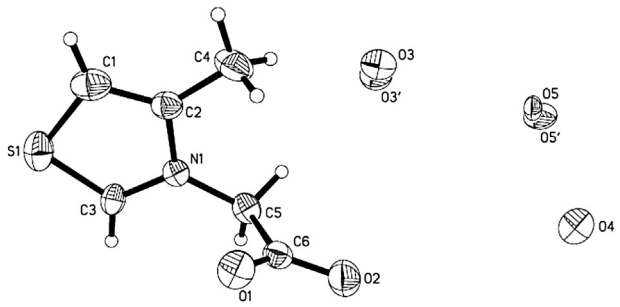

Fig. 3. A molecule inlaid in an unordered fragmentation of water.

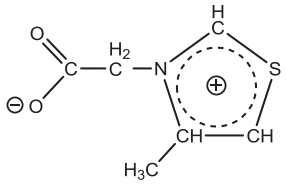

Fig. 4. The zwitterion is stabilized by charge delocalization.

H_{C5} in **1** is ca 0.4 ppm at lower field relative to **3**, and this difference can also be observed when we contrast **3** with **4** [21].

Through analysis, we raised that the change of charge distribution contributed to this phenomenon. In compound **1**, the existence of an H–O bond transfers the electron density of the carboxylic group to H, so that the charge distribution between the N^+ atom and the COO^- leans toward the latter, which eventually results in the electron density of C5 of **1** being weaker than **4**. Owing to every zwitterion sharing each H^+ moiety on average in compound **3**, the effect of H–O on shielding of C5 fades, which can well explain why the chemical shift of **3**–**4** is approximately half that of **1**–**4**.

2.2.3. IR spectroscopy

The change of structure can also be observed in FT-IR spectra (Fig. 8). Comparing **1** to **2**, and **3**, a number of weak/medium absorptions disappeared in the 2300–2800 cm^{-1-} range assigned to C–H…Br vibrations. This observation reveals that the interactions between bromine and cation in complex **2**, **3** have changed remarkably. In the spectrum of **2** and **4**, the absorption assigned to the ν(C=O) vibrations of carboxy in the spectrum of complex **1** at 1731 cm^{-1} vanish completely. However, the presence of strong bands at 1374 and 1368 cm^{-1} corresponding to a $\nu^s(COO^-)$ stretching vibration is indicative of the existence of COO^-, which can also be confirmed by the broad and intense band at about 1625 cm^{-1} caused mainly by the overlaying of the band assigned to ν(C=O) and ν(C=C) vibrations [16]. Given that the two units (RCOOH and RCOO) are linked via homoconjugated intermolecular hydrogen (O–H…O) in one complex, the intense bands at 1725 and 1374 cm^{-1} are all found in the spectrum of **3** [17].

We can also observe that the spectrum of **2** is nearly the same as **4**, which indicates that the organic part (zwitterion) of compound **2** is almost in the same chemical environment as **4** and also suggests that the Br^- as well as the Na^+ exists in a free state in compound **2**. This presumption can reasonably explain why the structure of compound **2** is barely in accordance with the elemental analysis.

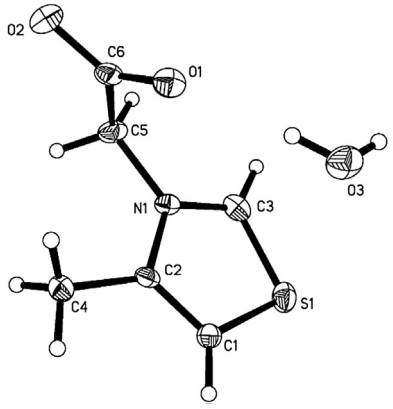

Fig. 5. The X-ray crystal structure of **4**, with displacement ellipsoids drawn at the 50% probability level.

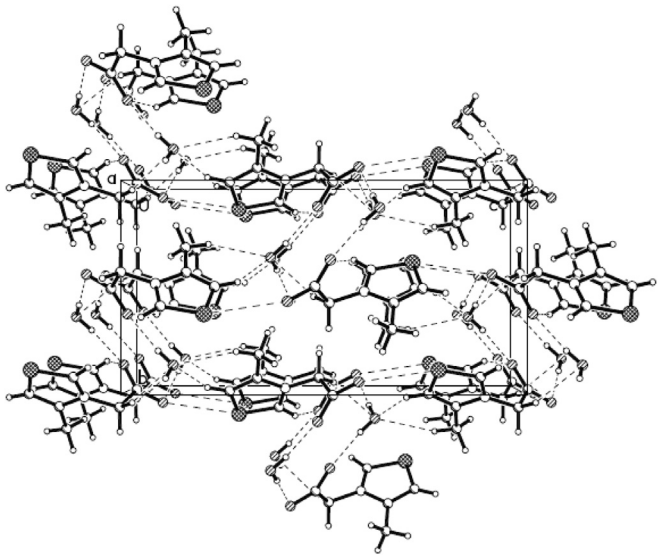

Fig. 6. The molecular packing and hydrogen-bonding scheme of **4**.

2.2.4. In situ IR

To study the change of COO^- and COOH in the reaction of preparing **4**,we attempted to use *in situ* IR to monitor the reaction system. The consumption of **1** and producing of **4** can be observed indirectly in figure above (Fig. 9), especially after the solvent spectrum is subtracted. At last, to our surprised, we found this reaction finished in several seconds.

It can be seen from the graph (Fig. 10) that the intensity of the absorption peak at 1731 cm^{-1}, the characteristic peak attributed to COOH, increase markedly after b point, and fade away after c point. This trend shows that the COOH vanish quickly after reacting with propylene oxide.

Contrary to the quickly vanishing of absorption peak at 1731 cm^{-1}, after c point, the intensity of the absorption peak at 1374 cm^{-1}, characteristic peak of COO^-, soared and then remained stable. This result indicates that the reaction is completed quickly and nearly all the COOH converted into COO^- in a very short time.

It was very interesting that from the graph (Fig. 10), we noted an obvious strengthen of the absorption peak at 1374 cm^{-1} (from b to c). This phenomenon implies the COO^- appeared after adding compound **1** due to the rapid dissociation of COOH of compound **1** into COO^- and H^+.

2.3. Druggability studies

In vivo efficacy has been confirmed by experiments performed in rats, showing that the increased arterial stiffness associated with diabetes can be reversed by a short treatment with the cross-link breaker 3-(carboxymethyl)-4-methylthiazol bromide sodium salt (**2**). However, owing to the free state of the Br^- and Na^+, the druggability of compound **2** is terrible.

Table 3
^{1}H chemical shifts (ppm) in DMSO of the protons in a series of betaines.

Compound	Ring protons		H_{C4}	H_{C5}
	H_{C1}	H_{C3}		
$C_6H_5SN^+CH_2COOH\cdot Br^-$ (**1**)	8.05	10.17	2.47	5.51
$C_6H_5SN^+CH_2COOHCOO^-CH_2N^+SC_6H_5\cdot Br^-$ (**3**)	7.99	10.09	2.43	5.16
$C_6H_5SN^+CH_2COONa\cdot Br^-$ (**2**)	7.90	9.98	2.41	4.79
$C_6H_5SN^+CH_2COO^-$ (**4**)	7.90	9.97	2.41	4.76

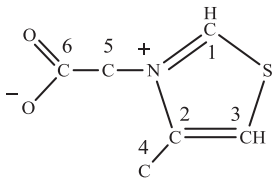

Fig. 7. Enumeration of the carbon atoms in the original nucleus.

We also found that the pH of the aqueous solution of compound **3** is lower than that of **2**, resulting from the breaking of the hydrogen bond when compound **3** is dissolved in protonic solvent. Because of this low pH, compound **3** may act as a severe alimentary tract irritant, which suggests that compound **3** is less likely to be applied as a drug.

Compound **4**, the product of structure optimizing based on compound **2**, displays outstanding properties in many fields, such as stability, solubility, synthesis and pH. Given the structural similarity between compound **4** and **2**, we anticipate that they will be similarly effective in breaking AGE cross-links, and relevant studies on the biological activity of compound **4** have been ongoing in our group. For all of the reasons, we conclude that compound **4** is a good candidate for success in druggability.

3. Conclusions

In the process of synthesizing the "cross-link breaker" 3-(carboxymethyl)-4-methylthiazol bromide sodium salt (**2**), three types of structures were obtained: sodium salt (**2**), dipolymer (**3**) and zwitterion (**4**). Through deliberate analysis with the method of single crystal X-ray diffraction, EA, FT-IR, ^{1}H NMR, ESI-MS and *in situ* IR, we came to the conclusion that the zwitterionic 3-(carboxymethyl)-4-methylthiazol (**4**) has obvious advantages in its physicochemical property and manufacturing feasibility that suggest it would be a promising drug in its zwitterion form.

4. Experimental

4.1. Materials

4-methylthiazole (SCRC), bromoacetic acid (Beijing chemicals), propylene (SCRC), sodium methanolate (Alfa) were used as received. Methanol (Beijing chemicals) and ethanol (Beijing chemicals) were dried and purified by standard methods.

4.2. Physical measurements

Microanalysis (C, H and N) was performed by the Analytical Center at Peking University, on an Elementar Vario Micro Cube CHN analyzer. Melting points were determined using an RY-1 apparatus and the thermometer is uncorrected. The infrared spectra were recorded on a NicoLET 6700 FT-IR Thermo Scientific spectrophotometer (KBr pellets, 4000–400 cm^{-1}). ^{1}H NMR spectra were recorded on a Varian Unity 400 MHz spectrometer. MS spectra were obtained using an Applied Biosystems API-150EX LC/MS mass spectrograph. 3D-FT-IR spectra were obtained from ReactIR™ iC10 with MCT Detector and a DiComp (Diamond) probe.

4.3. Synthesis

4.3.1. Synthesis of $C_6H_7BrNNaO_2S$ (**2**)

A solution of 4-methylthiazole (10 g, 0.10 mol) and 2-bromoacetic acid (15.2 g, 0.11 mol) was added to acetonitrile (70 ml), and then the reaction was heated under reflux for 8 h. The solution was filtered after cooling and the precipitate was washed with acetone. The dry white powder **1**,obtained above (17.8 g, yield 74%), and $NaHCO_3$ (6.28 g, 0.07 mol) dissolved in dry methanol (90 ml) and the whole solution was stirred for 5 h under ambient temperature before it was diluted with ethanol (130 cm^3). Colorless needlelike crystal of **2** (14.6 g, yield 75%) was obtained after 12 h. Mol. Wt. 260.1; M.p. 182 °C; MS: 158.2 $[M - Na - Br + H]^+$; ^{1}H NMR (400 MHz, DMSO-d_6 δ ppm), 9.98 (1H, d, $J = 2.4$ Hz), 7.90 (1H, d, $J = 1.2$ Hz), 4.79 (2H, s), 2.41 (3H, d, $J = 1.2$ Hz).

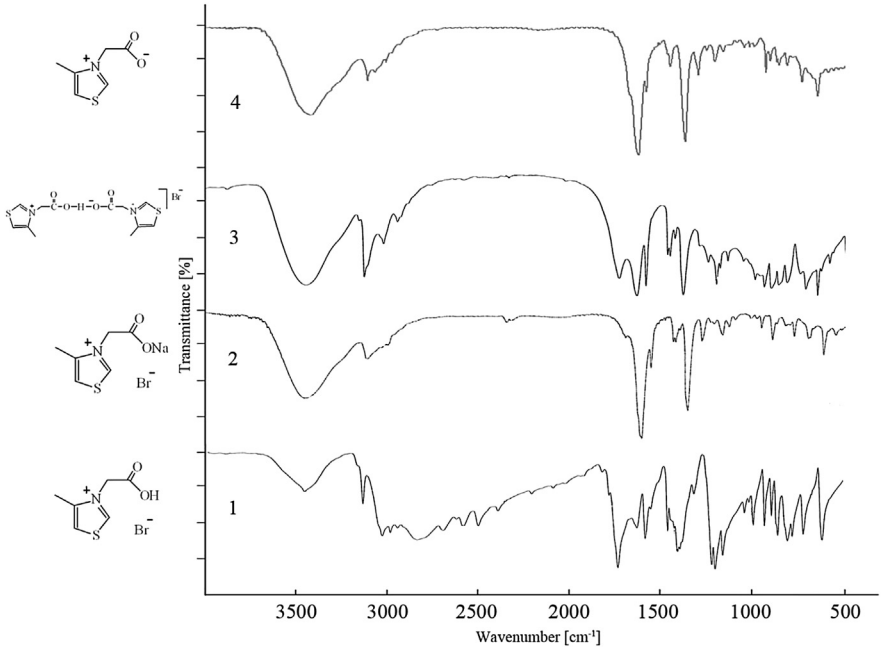

Fig. 8. Solid state FT-IR spectra in the different regions of **1**–**4**.

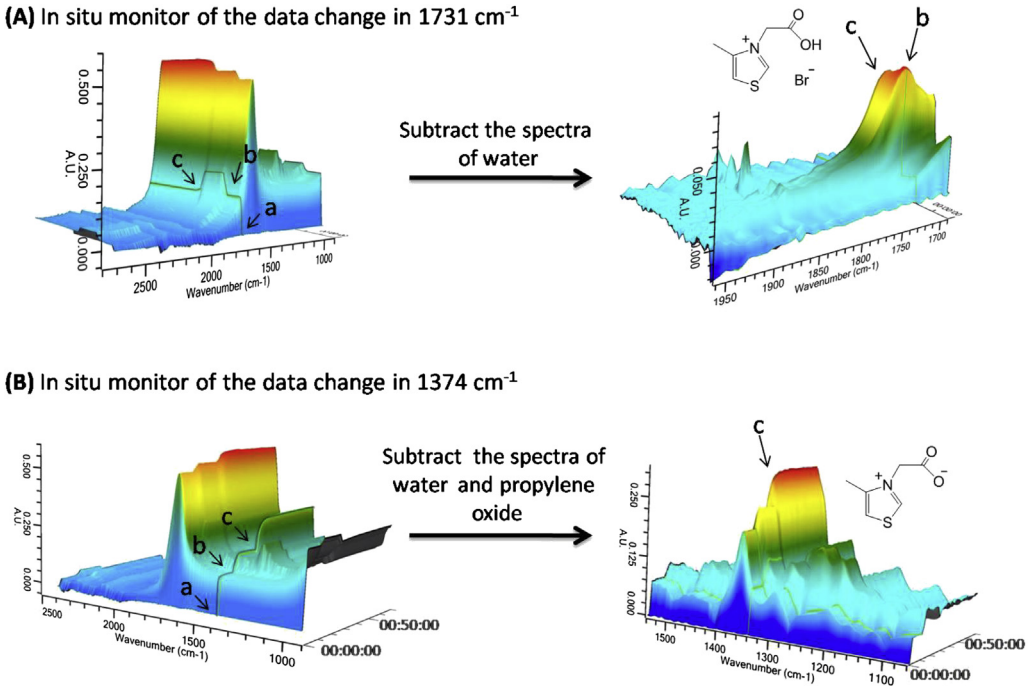

Fig. 9. (A), (B) 3D-FT-IR spectrum fragments for the reaction of compound **1** with propylene epoxide. The reaction was monitored from 0 to 70 min. a. Addition of water (4:00 min). b. Addition of compound **1** (13:00 min). c. Addition of propylene epoxide (27:00 min).

*4.3.2. Synthesis of $C_{12}H_{15}O_4N_2S_2Br$ (**3**)*

Compound **1** (10 g, 0.04 mol) with 1 equiv of CH_3ONa (2.3 g, 0.04 mol) in methanol (70 ml) was carried out at ambient temperature over 5 h. Acetone (100 ml) was added into the solvent and the precipitate was separated by filtration and then crystallized from methanol–ethanol. Colorless needlelike crystals of **3** (10.9 g, yield 81%) were obtained after 12 h. Mol. Wt. 439.4; M.p. 205 °C; ^{1}H NMR (400 MHz, DMSO-d_6 δ ppm), 10.09 (1H, d, J = 2.0 Hz), 7.99 (1H, d, J = 1.2 Hz), 5.16 (2H, s), 2.43 (3H, s); MS: 158 $[M - Br]^+$, 315 $[2M - H]^+$; Anal. calcd for $C_{12}H_{15}O_4N_2S_2Br$: C 36.46, H 3.82, N 7.09, Br 20.21. Found: C 36.27, H 4.01, N 7.15, Br 20.12%.

*4.3.3. Synthesis of $C_6H_7O_2NS$ (**4**)*

Compound **1** (10 g, 0.04 mol) was transformed into zwitterion form (**4**) by dissolving in water (50 ml) and adding three times the amount of propylene oxide (7.31 g, 0.12 mol). The solution was stirred at room temperature for 12 h, and the final pH was 7. Before the aqueous layer was evaporated to dryness, it was extracted with dichloromethane to remove bromohydrin, and then the remaining solid was recrystallized from ether–ethanol (1:3), giving the slightly yellowish crystalline powder of **4** (5.2 g, yield 78%). Mol. Wt. 157.2; M.p. 169 °C; ^{1}H NMR (400 MHz, DMSO-d_6 δ ppm), 9.97 (1H, d, J = 2.8 Hz), 7.90 (1H, d, J = 1.6 Hz), 4.76 (2H, s), 2.41 (3H, d, J = 0.8 Hz); ^{13}C NMR (Methanol-d_4), δ 12.98, 56.71, 121.47, 148.36, 169.71; MS: 158 $[M + H]^+$, 315 $[2M + H]^+$, 472 $[3M + H]^+$; Anal. calcd for $C_{12}H_{15}O_4N_2S_2Br$:C 45.85, H 4.49, N 8.91%. Found: C 45.65, H 4.75, N 8.83%.

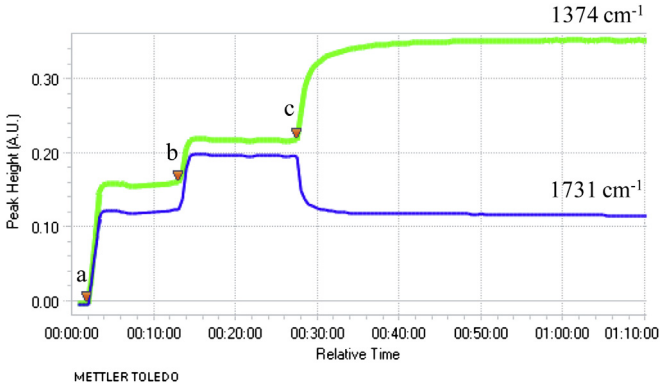

Fig. 10. Kinetic profile (peak height *vs* time) of the intensity of the absorption peak at 1374 cm^{-1} and 1731 cm^{-1} for the reaction of preparing compound **4**. a. Addition of water (4:00 min). b. Addition of compound **1** (13:00 min). c. Addition of propylene epoxide (27:00 min).

4.4. X-ray crystallography

Colorless prism-shaped crystals of **2** suitable for X-ray diffraction were obtained from a MeOH–EtOAC mixture at 20 °C, which was also suitable for the preparation of single Crystals of **3** and **4**.

X-ray diffraction data were collected on a Rigaku Saturn CCD area detector. Computations were done using graphite monochromatized Mo Kα radiation (λ = 0.71073 Å). Data reduction was performed with Crystalclear (Rigaku/MSC Inc., 2005). Structure solution and refinement were performed on PCs by means of SHELX-97 software package, and graphical representations of the structures were made with SHELXTL (Bruker, 2002). All three structures were solved by direct methods and refined with full-matrix least squares on F^2 using the SHELX-97 program package. All non-hydrogen atoms were refined anisotropically, while hydrogen atoms were located in subsequent different Fourier maps and their positional and isotropic displacement parameters were refined freely.

Acknowledgments

This work was supported by Grant No. 2011BAI18B01 to Wu Zhong from the National Key Technology R&D Program and Grant

No. 2009ZX09301-002 to Song Li from the National Key Technologies R&D Program for New Drugs.

Appendix A. Supplementary data

Supplementary data related to this article can be found at http://dx.doi.org/10.1016/j.ejmech.2013.07.033.

References

[1] N. Rahmah, A.K. Anuar, N.A. A'Shikin, B.H. Lim, R. Mehdi, B. Abdullah, M.N. Zurainee, Res. Commun. 250 (1998) 586–588.
[2] E. Boulanger, M.P. Wautier, J.L. Wautier, B. Boval, Y. Panis, N. Wernert, P.M. Danze, P. Dequiedt, Kidney Int. 61 (2002) 148–156.
[3] G.F. Avendano, R.K. Agarwal, R.I. Bashey, M.M. Lyons, B.J. Soni, G.N. Jyothirmayi, T.J. Regan, Diabetes 48 (1999) 1443–1447.
[4] Y. Imanaga, N. Sakata, S. Takebayashi, A. Matsunaga, J. Sasaki, K. Arakawa, R. Nagai, S. Horiuchi, H. Itabe, T. Takano, Atherosclerosis 150 (2000) 343–355.
[5] S. Vasan, X. Zhang, A. Kapurniotu, J. Bernhagen, S. Teichberg, J. Basgen, D. Wagle, D. Shih, I. Terlecky, R. Bucala, A. Cerami, J. Egan, P. Ulrich, Nature 382 (1996) 275–278.
[6] D.A. Kass, E.P. Shapiro, M. Kawaguchi, A.R. Capriotti, A. Scuteri, R.C. deGroof, E.G. Lakatta, Circulation 104 (2001) 1464–1470.
[7] P.V. Vaitkevicius, M. Lane, H. Spurgeon, D.K. Ingram, G.S. Roth, J.J. Egan, S. Vasan, D.R. Wagle, P. Ulrich, M. Brines, J.P. Wuerth, A. Cerami, E.G. Lakatta, Proc. Natl. Acad. Sci. U S A 98 (2001) 1171–1175.
[8] D. Susic, J. Varagic, J. Ahn, E.D. Frohlich, Curr. Drug Targets Cardiovasc. Haematol. Disord. 4 (2004) 97–101.
[9] M. Asif, J. Egan, S. Vasan, G.N. Jyothirmayi, M.R. Masurekar, S. Lopez, C. Williams, R.L. Torres, D. Wagle, P. Ulrich, A. Cerami, M. Brines, T.J. Regan, Proc. Natl. Acad. Sci. U S A 97 (2000) 2809–2813.
[10] B.H. Wolffenbuttel, C.M. Boulanger, F.R. Crijns, M.S. Huijberts, P. Poitevin, G.N. Swennen, S. Vasan, J.J. Egan, P. Ulrich, A. Cerami, B.I. Levy, Proc. Natl. Acad. Sci. U S A 95 (1998) 4630–4634.
[11] S. Li, H. Cui, J.H. Xiao, W. Zhong, L.L. Wang, G. Cheng. US Patent 7799813 (2007).
[12] S. Li, W. Zhong, L.L. Wang, H. Cui, J.H. Xiao, G. Cheng. EP Patent 2341048 (2003).
[13] A.A. Danopoulos, P. Cole, S.P. Downing, D. Pugh, J. Organomet. Chem. 693 (2008) 3369–3374.
[14] P. Nockemann, B. Thijs, T.N. Parac-Vogt, K. Van Hecke, L. Van Meervelt, B. Tinant, I. Hartenbach, T. Schleid, V.T. Ngan, M.T. Nguyen, K. Binnemans, Inorg. Chem. 47 (2008) 9987–9999.
[15] J.D. Holbrey, W.M. Reichert, M. Nieuwenhuyzen, O. Sheppard, C. Hardacre, R.D. Rogers, Chem. Commun. (Camb.) (2003) 476–477.
[16] P. Barczyński, A. Komasa, M. Ratajczak-Sitarz, A. Katrusiak, A. Huczyński, B. Brzezinski, J. Mol. Struct. 876 (2008) 170–176.
[17] Z.F. Fei, D.B. Zhao, T.J. Geldbach, R. Scopelliti, P.J. Dyson, J. Chem. Eur. (2004) 4886–4893.
[18] Y.P. Tian, L. Li, Y.H. Zhou, P. Wang, H.P. Zhou, J.Y. Wu, Crystal Growth Des. 9 (2009) 1499–1504.
[19] L.P. Zhang, H.B. Song, Q.M. Wang, T.C.W. Mak, Polyhedron 22 (2003) 811–818.
[20] Y.M. Song, X.Q. Yao, T. Deng, J.X. Wu, Q. Wu, Chem. Pap. 60 (2006) 302–305.
[21] D.S. Zofia, D. Ewa, S. Mirosław, Magn. Reson. Chem. 38 (2000) 43–50.